Deflection of Superelastic Shape Memory Alloy RC Beams: Assessment of Existing Models

Y.I. Elbahy

M.E.Sc. Candidate, Department of Civil and Environmental Engineering,

The University of Western Ontario

London, Ontario, Canada, N6A 5B9

M.A. Youssef

Associate Professor, Department of Civil and Environmental Engineering,

The University of Western Ontario

London, Ontario, Canada, N6A 5B9

M. Nehdi

Professor, Department of Civil and Environmental Engineering,

The University of Western Ontario

London, Ontario, Canada, N6A 5B9

Corresponding Author: **M.A. Youssef**

Email: youssef@uwo.ca,

Fax: 519-661-3779,

Phone: 519-661-2111, Ext: 88661

Word Count: (8,860)

ABSTRACT: This paper investigates the load-deflection behaviour of Shape Memory Alloy (SMA) Reinforced Concrete (RC) beams through a parametric study. The effects of the cross-section height, cross-section width, reinforcement ratio, reinforcement modulus of elasticity, and concrete compressive strength were considered. The sectional analysis methodology was adopted to predict the moment-curvature relationship for the considered sections. Deflection was then estimated using the moment-area method. The applicability of this method for SMA RC beams was demonstrated through comparisons with available experimental results. Based on the results of the parametric study, an assessment of the available models for deflection analysis of SMA RC beams was conducted. The accuracy and reliability of the different models were evaluated and suitable models were recommended. A companion paper provides the development of an artificial intelligence based model that can predict the deflection of SMA RC beams more accurately than existing models.

Keywords: reinforced concrete, shape memory alloys, moment-curvature, load-deflection, sectional analysis, moment-area method.

INTRODUCTION

Reinforced concrete structures are generally designed to support predefined sets of loads specified by design standards. However, when subjected to severe loading, such structures may undergo permanent damage. For instance, under a severe earthquake, the steel reinforcement would yield and permanent deformations are expected. Repairing damaged RC structures might not be feasible; indeed they may need to be demolished and replaced. Thus, there is a need for smart structures that can adjust to unexpected loading. Such structures can be achieved by utilizing smart materials such as Shape Memory Alloys (SMAs) (Alam et al. 2007).

Shape memory alloys are special alloys that can undergo large deformations and return to their undeformed shape upon unloading or by heating. Superelasticity, shape memory effect, and the behaviour under cyclic loading are unique properties of SMAs which make them distinct from other metals and alloys (Janke et al. 2005). These unique properties can be utilized to achieve smart structures with properties that can adjust to the applied loading. The potential of using SMA in civil engineering applications is increasing. These applications include using SMA as bracing members in frames (Mazzolani et al. 2004), prestressing tendons for concrete elements (Maji and Negret 1998; El-Tawil and Ortega-Rosales 2004), anchors for columns (Tamai et al. 2003), damping devices (Clark et al. 1995; Krumme et al. 1995), bridge restrainers (DesRoches and Delemont 2002), and primary reinforcement for concrete structures (Elbahy et al. 2009; Saiidi et al. 2007). Although many types of SMAs have been proposed, superelastic Ni-Ti (nickel-titanium based SMA) was found to be the most appropriate for civil engineering applications. It has high recoverable strain, high durability, and good resistance to corrosion.

The design of a structure should generally satisfy two basic criteria; strength and serviceability. While the strength criteria allow the structure to safely support the design loads over its specified service life, serviceability requirements ensure satisfactory service life performance. These serviceability requirements include limits on allowable deflection since excessive deflection is often perceived as failure. In addition, excessive deflection can lead to damage of non-structural elements.

Deflection calculations of concrete flexural members depend on the moment of inertia. Due to cracking, it might vary along the length of the member. An average value, effective moment of inertia, is usually used. There are a number of available methods to calculate the effective moment of inertia for beams reinforced with either steel or Fibre Reinforced Polymers (FRP) including: Branson (1963), Benmokrane et al. (1996), Brown and Bartholomew (1996), Toutanji and Saafi (2000), ISIS design manual (2001), ACI 440.1R-03 (2003), ACI 440.1R-04 (2004), and Bischoff (2007b).

In this paper, the sectional analysis methodology is used to predict the moment-curvature relationship of SMA RC sections. The moment-area method is then utilized to calculate the deflection of SMA RC beams. The effects of the cross-section dimensions, reinforcement ratio, concrete compressive strength, and modulus of elasticity of SMA on the deflection of RC beams are evaluated through a parametric study. The results from the parametric study are used to check the validity of available models in the literature for predicting the effective moment of inertia of SMA RC beams.

MATERIALS MODELS AND SECTIONAL ANALYSIS

Concrete stress-strain model

The behaviour of concrete in compression is assumed to follow the stress-strain model of Scott et al. (1982), Fig. 1-(a) and Eq. [1]. Although relatively more accurate and complex models have been introduced, the Scott et al. (1982) model offers a good balance between simplicity and accuracy. A value of 0.0035 is assigned to the ultimate concrete strain, $\varepsilon_{cu,}$ at which the concrete is assumed to disintegrate (CSA-A23.3-04 2004).

[1a] $$f_c = K_h f_c^{'}\left[2.0\left(\frac{\varepsilon_c}{0.002}\right)-\left(\frac{\varepsilon_c}{0.002}\right)^2\right] \qquad 0 \le \varepsilon_c \le 0.002$$

[1b] $$f_c = K_h f_c^{'}\left[1 - Z(\varepsilon_c - 0.002)\right] \qquad \varepsilon_c \ge 0.002 \quad and \quad f_c \ge 0.2 f_c^{'}$$

[1c] $$Z = \frac{0.5}{\frac{3 + 0.29 f_c^{'}(\text{MPa})}{145 f_c^{'}(\text{MPa}) - 1000} + 0.75\rho_{stirrups}\sqrt{\frac{h'}{S_h}} - 0.002K_h}$$

[1d] $$K_h = 1 + \frac{\rho_{stirrups}\ f_y}{f_c^{'}}$$

where: f_c = concrete compressive stress, Z = slope of compressive strain softening branch, ε_c = concrete compressive strain, K_h = confinement factor, $h^{'}$ = width of the concrete core measured to the outside of ties, S_h = centre-to-centre spacing of the ties or hoop sets, $\rho_{stirrups}$ = ratio of

volume of stirrups to volume of concrete core measured to outside of the stirrups, and f_y = reinforcement yielding stress.

The model of Stevens et al. (1987) was utilized to describe the concrete tensile behaviour. As shown in Fig. 1-(b), the concrete is assumed to behave linearly until reaching the cracking stress, f_{cr}. Once the concrete cracks, the softening branch given by Stevens et al. (1987), Eq. [2], is used to describe the post-cracking behaviour of concrete. The simplification proposed by Youssef and Ghobarah (1999) involving eliminating the effect of the amount of reinforcement and its inclination is adopted.

$$f_t = f_{cr}\left[0.95 \text{ x } e^{-1000 \text{ x } (\varepsilon_c - \varepsilon_{cr})} + 0.05\right] \qquad \varepsilon_c \geq \varepsilon_{cr} \qquad [2]$$

where: f_t = concrete tensile stress, f_{cr} = concrete cracking stress, and ε_{cr} = concrete cracking strain.

SMA stress-strain model

The stress-strain relationship of Ni-Ti (Nickel-Titanium based SMA) consists of four linear branches that are connected by smooth curves (Alam et al. 2007). To simplify the modeling process, these smooth curves are ignored and the linear branches are assumed to intersect, Fig. 1-(c). The Ni-Ti alloy behaves elastically with a modulus of elasticity $E_{cr\text{-}SMA}$ until reaching the SMA critical stress $f_{cr\text{-}SMA}$, which represents the start of the martensite stress induced transformation. Once the strain, ε_{SMA} exceeds the SMA critical strain, $\varepsilon_{cr\text{-}SMA}$, the modulus of

elasticity E_{p1} decreases to about 10% to 15% of $E_{cr\text{-}SMA}$. For strains above the martensite stress induced strain ε_{p1}, the material regains part of its stiffness because of the phase transformation. The new modulus of elasticity, E_{p2} reaches about 50% to 60% of $E_{cr\text{-}SMA}$. The last linear branch starts at the real yielding of the Ni-Ti ($f_{y\text{-}SMA}$). The material softens again and the modulus of elasticity $E_{u\text{-}SMA}$ reaches a value as low as 3% to 8% of $E_{cr\text{-}SMA}$.

Sectional analysis

The moment-curvature analysis is conducted using a FORTRAN program developed by the authors. The program is based on the fibre model methodology (Youssef and Rahman 2007; Elbahy et al. 2009). This methodology depends on dividing the section into a finite number of layers as shown in Fig. 1-(d).. Using the predefined stress-strain models for the materials and taking into consideration section equilibrium and kinematics, the mechanical behaviour of the section can be analyzed. Assumptions applicable to steel RC sections and included in the analysis are: (i) plane sections remain plane; and (ii) perfect bond exists between concrete and the reinforcement.

The studied cross-sections in this paper are divided into a finite number of layers based on the cross-section height. The curvature is incrementally applied while keeping the axial load equal to zero. The analysis continues until the top concrete fibre reaches the crushing strain or the reinforcing bars reach their rupture strain. The relationship between the axial strain, the curvature, the applied moment, and the axial force can be written as:

$$[3] \qquad \begin{pmatrix} \Delta M \\ \Delta P \end{pmatrix} = \begin{pmatrix} \sum E_i \ A_i \ y_i^2 & -\sum E_i \ A_i \ y_i \\ -\sum E_i \ A_i \ y_i & \sum E_i \ A_i \end{pmatrix} X \begin{pmatrix} \Delta\phi \\ \Delta\varepsilon_c \end{pmatrix}$$

where: ΔM =incremental increase in the moment acting on the section, ΔP = incremental increase in the axial load force acting on the section (equal to zero), $\Delta\Phi$ = incremental increase in section curvature, $\Delta\varepsilon_c$ = incremental increase in the section central axial strain, E_i = modulus of elasticity of layer i, A_i = area of layer i, and y_i = distance between the centre of gravity of layer i and the centre of gravity of the concrete section.

DEFLECTION CALCULATION USING MOMENT-AREA METHOD

One of the most accurate methods for estimating flexural deformations of RC members is based on integrating the curvature distribution using the moment-area method. The analysis starts by drawing the bending moment diagram of the studied beam, and utilizing the moment-curvature relationship to evaluate the corresponding curvature distribution. Rotations can be calculated by integrating the area under the curvature diagram, while deflections can be computed by calculating the first moment of area of the integrated area.

To check the accuracy of using the moment-area method in the deflection calculations of SMA RC members, the two beam-column joint specimens tested by Youssef et al. (2008) were utilized. One of the joints was reinforced with regular steel reinforcement (JBC1), while the

other (JBC2) was reinforced with steel in conjunction with SMA in the plastic hinge region of the beam.

Figure 2-(a) illustrates the elevation and cross-sections of JBC1 and JBC2. The columns of the two joints have the same cross-section dimensions (250 mm x 400 mm) and reinforcement (4-M20 longitudinal bars and M10 stirrups spaced at 80 mm in the joint region and 115 mm elsewhere). The beams of the two joints, JBC1 and JBC2, have similar cross-section dimensions (250 mm x 400 mm) and amount of transverse reinforcement (M10 spaced at 80 mm in the plastic hinge region and 110 mm in the remaining length of the beam). The Ni-Ti SMA bars have a length of 450 mm and are connected to steel bars using mechanical couplers. Figure 2-(b) shows the stress-strain relationship of the used Ni-Ti alloy. It has a critical stress of 401 MPa and a critical strain of 0.75%. The properties of the used concrete, longitudinal steel, and transverse steel are summarized in Table 1. A constant axial load of 350 kN is applied at the top of the column for both specimens. The bottom of the columns is hinged. Roller support is used at the top of the columns. A reversed vertical quasi-static cyclic loading is applied at the beam tip.

The vertical deformation at the beam tip can be divided into three components that are associated with: (i) column flexural rotation; (ii) beam-column joint shear deformation; and (iii) beam flexural rotation. The column behaved as an elastic member and had no cracks. Its rotation at the beam-column joint reached an estimated maximum value of 0.00018 rad. The joint was detailed according to the current seismic standards and its shear deformations reached a maximum value of 0.00045 rad. The maximum contribution of those two components to the beam tip deformation

is 1.14 mm which is about 3.00% of the maximum measured deformation. Because of their insignificant contribution, it was decided to assume that the beam is fully restrained at the joint.

Moment-curvature analysis was performed using the sectional analysis methodology. Confinement was accounted for in the concrete model. Figure 3-(a) illustrates the moment-curvature relationships for the SMA and the steel RC sections for stirrups spacing of 80 mm. The curvature distribution was drawn along the beam length based on the load level and the reinforcement type, Fig. 3-(b). The deflection was obtained by calculating the first moment of the integrated areas under the curvature diagram. Figure 3-(c) shows the load-deflection relationships obtained from the moment-area method for both JBC1 and JBC2. Good agreement between experimental and analytical results can be observed.

DEFLECTION OF STEEL-REINFORCED CONCRETE MEMBERS

As design of RC members might be controlled by deflection, current design standards require either limiting the member span-to-depth ratio or ensuring that the calculated deflections do not exceed specified limits. Deflection calculation of concrete flexural members depends on the cross-section moment of inertia, concrete tensile stiffening, and load level. At a crack location, the moment of inertia of the cross-section equals the cracked moment of inertia, I_{cr}. The average inertia considering the cracked and un-cracked sections is the effective moment of inertia (I_e). Figure 4 shows moment-curvature relationships for a typical section assuming un-cracked section (I_g), cracked section (I_{cr}), and a cracked flexural member (I_e). There are a number of methods in the literature to calculate the effective moment of inertia. The Canadian Standards

(CSA-A23.3-04 2004) use the equation proposed by Branson (1963), Eq. [4], for this purpose. This equation represents a gradual transition from the un-cracked cross-section moment of inertia, I_g, to the cracked moment of inertia, I_{cr}, based on the ratio of the applied moment, M_a, to the cracking moment, M_{cr}.

$$I_e = \left(\frac{M_{cr}}{M_a}\right)^3 I_g + \left[1 - \left(\frac{M_{cr}}{M_a}\right)^3\right] I_{cr} \qquad \leq I_g \tag{4}$$

Branson's equation is empirical and is based on test results for steel RC beams having a reinforcement ratio between 1% and 2%. Scanlon et al. (2001) and Gilbert (2006) have shown that this equation underestimates the deflection of lightly reinforced concrete members. Rangan and Sarker (2001) reported that Branson's equation gives a reasonable estimate of the bending stiffness provided that the reinforcement ratio is greater than 0.5%. For lower reinforcement ratios, it was found that Branson's equation highly overestimates the cross-section stiffness, and thus significantly underestimates the member deflection (Bischoff 2007a). To overcome this problem, the Australian Standards (AS 3600 2001) proposed limiting the value of I_e to 0.6 I_g if the reinforcement ratio is less than 0.5%.

Replacing conventional steel reinforcement with new materials having different mechanical properties, such as SMA, requires checking the validity of the Branson's equation, Eq. [4]. Similar studies have been conducted for FRP RC members (ACI 440.1R-03 2003; ACI 440.1R-03 2004; Bischoff 2007a). Since the modulus of elasticity of FRP is lower than that of steel and comparable to that of SMA in the austenite region of the stress-strain relationship (up to f_{cr}),

modifications to the Branson's equation proposed to predict the deflection of FRP RC members are summarized below.

MODIFICATIONS TO BRANSON'S EQUATION

Benmokrane et al. (1996) proposed modifying Branson's equation by multiplying its two terms by two constants which were proposed based on load-deflection results obtained from four experimentally tested FRP RC beams, Eq. [5]. The beams had reinforcement ratios varying between 0.56% and 1.10%, and FRP modulus of elasticity, E_{FRP}, varying between 40,000 MPa and 45,000 MPa.

$$[5] \qquad I_e = \frac{1}{7}\left(\frac{M_{cr}}{M_a}\right)^3 I_g + 0.84\left[1-\left(\frac{M_{cr}}{M_a}\right)^3\right] I_{cr} \qquad \leq I_g$$

Brown and Bartholomew (1996) proposed to replace Branson's equation with Eq. [6], which was developed based on regression analysis of experimental results of eight Glass Fibre Reinforced Polymer (GFRP) RC beams. The beams had different reinforcement ratios ($0.38\% \leq \rho_{FRP} \leq 1.38\%$) and different modulus of elasticity values ($40{,}000 \text{ MPa} \leq E_{FRP} \leq 45{,}000 \text{ MPa}$).

$$[6] \qquad I_e = \left(\frac{M_{cr}}{M_a}\right)^5 I_g + \left[1-\left(\frac{M_{cr}}{M_a}\right)^5\right] I_{cr} \qquad \leq I_g$$

Tountanji and Saafi (2000) modified the equation of Brown and Bartholomew (1996) to account for the effect of E_{FRP} and the FRP reinforcement ratio, (ρ_{FRP}) Eq. [7]. These modifications were based on test results of six FRP RC beams. The beams had ρ_{FRP} varying between 0.52% and 1.10% and a constant E_{FRP} of 40,000 MPa.

[7a] $$I_e = \left(\frac{M_{cr}}{M_a}\right)^m I_g + \left[1 - \left(\frac{M_{cr}}{M_a}\right)^m\right] I_{cr} \qquad \leq I_g$$

[7b] $$\text{where} \quad m = 6 - 10\frac{E_{FRP}}{E_s}\rho, \qquad \frac{E_{FRP}}{E_s}\rho_{FRP} < 0.3$$

$$m = 3.0 \qquad \frac{E_{FRP}}{E_s}\rho_{FRP} \geq 0.3$$

where: E_s is the modulus of elasticity of steel.

The ISIS design manual (2001) suggested an effective moment of inertia, Eq. [8], which is different in form than the previous equations. It is based on equations given by CEB-FIP (1990) and validated by Ghali et al. (2001) using the experimental results of Hall (2000) and Hall and Ghali (1997).

[8] $$I_e = \frac{I_T\, I_{cr}}{I_{cr} + \left[1 - 0.5\left(\frac{M_{cr}}{M_a}\right)^2\right](I_T - I_{cr})} \qquad \leq I_g$$

where: I_T is the un-cracked moment of inertia of the transformed section.

ACI 440.1R-03 (2003) used a similar form to the Branson's equation. However, a reduction factor (β) was used to reduce the effective moment of inertia, Eq. [9]. This reduction factor was dependent on the modulus of elasticity of the FRP.

[9a] $$I_e = \left(\frac{M_{cr}}{M_a}\right)^3 \beta\, I_g + \left[1 - \left(\frac{M_{cr}}{M_a}\right)^3\right] I_{cr} \qquad \leq I_g$$

[9b] $$\text{where} \quad \beta = \alpha \left(1 + \frac{E_{FRP}}{E_s}\right)$$

where: α is a bond dependent coefficient. It can be taken as 0.5.

Several attempts have been made to modify Eq. [9] since it was found to underestimate the deflection of FRP RC members. For instance, Yost et al. (2003) argued that the accuracy of the I_e equation given by ACI 440.1R-03 (2003) is mainly dependent on the reinforcement ratio. A modification to the bond dependent coefficient α was proposed, Eq. [10].

[10] $$\alpha = 0.064\left(\frac{\rho_{FRP}}{\rho_b}\right) + 0.13$$

ACI 440.1R-04 (2004) proposed a new expression for β, Eq. [11]. The new value for β is mainly dependent on the section reinforcement ratio, ρ_{FRP}.

[11] $$\beta = \frac{1}{5}\left(\frac{\rho_{FRP}}{\rho_b}\right) \qquad \leq 1.0$$

The formulation of Branson's equation is based on the assumption of having two springs representing the un-cracked and cracked moments of inertia arranged in parallel. Bischoff (2007a) argued that arranging the springs in series properly models the tension stiffening of concrete, and thus overcomes the poor predictions of Branson's equation in case of low values for the reinforcement ratio or the modulus of elasticity. The proposed model by Bischoff (2007b), Eq. [12], was calibrated for beams having $\frac{I_g}{I_{cr}}$ equal to 2.2 similar to the case of the Branson's equation. The model has been shown to be appropriate for steel RC members having a low reinforcement ratio, and for FRP RC members.

[12] $$\frac{1}{I_e} = \left(\frac{M_{cr}}{M_a}\right)^2 \frac{1}{I_g} + \left[1 - \left(\frac{M_{cr}}{M_a}\right)^2\right] \frac{1}{I_{cr}} \qquad \geq \frac{1}{I_g}$$

PARAMETRIC STUDY

A parametric study is conducted to study the deflection behaviour of flexural concrete beams reinforced with SMA. The parametric study is carried out for simply supported beams loaded with two point loads at third span. The studied parameters include the cross-section dimensions, reinforcement ratio, concrete compressive strength, and the modulus of elasticity of SMA. Details of the analyzed sections are summarized in Table 2. The moment-area method is used to

calculate the deflection of the studied beams. All sections show a high reduction in the cross-section stiffness after concrete cracking. The results of the parametric study are used to evaluate the applicability of the available models presented in the previous section for estimating the deflection of SMA RC sections.

RESULTS AND DISCUSSION

A number of deflection levels representing expected service load conditions are chosen. The corresponding moment levels are 1.1 M_{cr}, 1.5 M_{cr}, 2.0 M_{cr}, and 3.0 M_{cr}. Figure 5 shows the deflection values obtained analytically using the moment-area method for each of the studied sections at the chosen load levels and plotted versus the deflection predicted using the models given in the previous section. A noticeable difference between the predictions of the different models can be observed. The effects of the studied parameters on the load-deflection behaviour of SMA RC beams are discussed in this section. Bischoff's model and Branson's equation are included in the discussion.

Figure 6-(a) illustrates the load-deflection relationship versus the cross-section height. Upon cracking, a noticeable decrease in I_e is observed for all studied sections. Branson's equation is found to overestimate the flexural stiffness resulting in an underestimation of the deflection. The difference between the results obtained using Branson's equation and those obtained using the moment-area method is found to have 20% AD ± 19% SD, 41% AD ± 25% SD, and 60% AD ± 30% SD for h = 400 mm, h = 600 mm, and h = 800 mm, respectively (AD is the average difference and SD is the standard deviation). The model proposed by Bischoff (2007b) is found

to underestimate the deflection (17% AD ± 16% SD) for one of the beams (h = 800 mm). For the other two beams, good agreement was observed between Bischoff's model and the moment-area results (4% AD ± 5% SD for h = 400 mm, 7% AD ± 12% SD for h = 600 mm).

The effect of varying the cross-section width on the load-deflection relationship is illustrated inFig. 6-(b). After cracking of concrete, varying the cross-section width does not have a significant effect on I_e. Bischoff's model is found to result in an acceptable load-deflection relationship for b = 250 mm (6% AD ± 12% SD). However, the model does not provide accurate prediction of the deflection for 400 mm width (19% AD ± 18% SD) and 600 mm width (36% AD ± 22% SD). Branson's equation is found to significantly underestimate the deflection of all the studied beams (63% - 84% AD ± 18% - 22% SD).

The difference between the effective moment of inertia values obtained from Branson's equation and those obtained from the moment-curvature analysis is found to significantly decrease with the increase in the reinforcement ratio, Fig. 6-(c). Good agreement between the deflections obtained from Branson's equation and those obtained from the moment-area method is observed for ρ = 1.20% and ρ = 1.77% (12% AD ± 14% SD for ρ = 1.2%, 4% AD ± 5% SD for ρ =1.77%). Branson's equation is unable to accurately predict the deflection for ρ = 0.4% or ρ = 0.8% (78% AD ± 39% SD). Bischoff's model is found to underestimate the member deflection for ρ = 0.4% (30% AD ± 22% SD). For other reinforcement ratios, Bischoff's model gives good estimates of the deflection (6% AD ± 6% SD).

The effect of the modulus of elasticity of SMA on the load-deflection behaviour is found to be significant, Fig. 6-(d). Branson's equation predicts the effective moment of inertia with suitable accuracy (17% AD ± 12% SD) for beams having a relatively high modulus of elasticity value (E_{SMA} = 65,000 MPa). For relatively low modulus of elasticity values, a notable difference between the deflections predicted using Branson's equation and those obtained from the moment-area method is observed (52% AD ± 29% SD). Bischoff's model provides conservative predictions for E_{SMA} = 45,000 MPa and E_{SMA} = 65,000 MPa. However, for E_{SMA} = 30,000 MPa, the model is found to underestimate the beam deflection (15% AD ± 18% SD), especially for load levels close to the cracking load.

Varying the concrete compressive strength within the normal concrete strength range does not have a significant effect on the load-deflection behaviour of SMA RC beams, Fig. 6-(e). Branson's equation significantly overestimates the flexural stiffness of the studied beams (27% AD ± 17% SD for f'_c=20 MPa and 51% AD ± 20% SD for f'_c=55 MPa). Bischoff's model is found to have poor agreement with the moment-area method at loads close to the cracking load.

ACCURACY OF DEFLECTION MODELS

The accuracy of the previously described models in predicting the deflection of SMA RC members is evaluated in this section. Figure 7 shows the deflection calculated using the moment-area method plotted versus the deflection obtained from the different models at load levels corresponding to 1.1 M_{cr}, 1.5 M_{cr}, 2.0 M_{cr}, and 3.0 M_{cr}. The reliability and accuracy of each model are evaluated using the root mean square error (*RMSE*), Eq. [13], and the average

algebraic error (*AGE*), Eq. [14]. The *RMSE* and *AGE* results for all models are summarized in Fig. 8.

$$[13] \qquad RMSE = \frac{1}{n} \sum_{i=1}^{n} \sqrt{\left(\delta_{\text{Analitical}} - \delta_{\text{Model}}\right)^2}$$

$$[14] \qquad AGE = \frac{1}{n} \sum_{i=1}^{n} \frac{\left(\delta_{\text{Analitical}} - \delta_{\text{Model}}\right)}{\delta_{\text{Analitical}}}$$

Figure 7shows that the model proposed by Benmokrane et al. (1996) is not conservative for cases corresponding to low reinforcement ratios ($\rho \leq 0.4\%$). For other reinforcement ratios, the model is conservative. *RMSE* of 9.36 and *AGE* of -0.52 are obtained for this model. The model proposed by Brown and Bartholomew (1996) is found to underestimate deflection for members having reinforcement ratios up to 0.80%. The *RMSE* is found to be 6.80 for this model.

The model proposed by ACI 440.1R-03 (2003), which is mainly dependent on the reinforcement modulus of elasticity, is found to be in poor agreement with corresponding deflection values obtained using the moment-area method for reinforcement ratios up to 1.20%. *RMSE* of 8.64 is obtained for this model. The deflections calculated using the ACI 440.1R-04 (2004) are significantly higher than those obtained from the moment-area method (*AGE* = 0.57; *RMSE* = 7.00). The model proposed by Yost et al. (2003) is found to be conservative except for beams having low reinforcement ratio ($\rho \leq 0.4\%$) or low modulus of elasticity (E = 30,000 MPa). *AGE* and *RMSE* for this model are -0.20 and 5.11, respectively.

The ISIS design manual (2001) achieves smaller *RMSE* with a value of 4.60. It generally overestimates the beams' deflection with an *AGE* value of -0.16. Bischoff's model shows the smallest *RMSE* (3.85). However, Bischoff's model is found to slightly underestimate the beams' deflection (*AGE* = 0.08). The highest *RMSE* is obtained for Branson's equation (*RMSE* = 11.5) as a result of the significant overestimation of the flexural stiffness. An *AGE* of 0.38 is calculated in the case of Branson's equation, which indicates the general underestimation of the member deflection.

Based on the calculated deflection values for different parameters, and the *RMSE* and *AGE*, Bischoff's model provides the best predictions among the eight models considered herein for beams having reinforcement ratios greater than 0.6%. For lightly reinforced concrete beams ($\rho \leq$ 0.6%), the ISIS design manual (2001) gives better predictions for most of the studied sections.

CONCLUSIONS

This paper investigates the load-deflection behaviour of SMA RC beams through a parametric study. The effects of the cross-section height and width, reinforcement ratio, reinforcement modulus of elasticity, and concrete compressive strength are evaluated. Deflections are calculated based on the moment-area method. The accuracy of using this method with SMA RC members is validated through comparisons with available experimental results. The equation provided by the Canadian Standards, CSA-A23.3-04 (2004), for deflection calculation is found to significantly overestimate the flexural stiffness of SMA RC members, and thus significantly underestimates their deflection. This is expected because of the significant difference between

the modulus of elasticity of SMA and that of steel. Other researchers have made similar observations for FRP RC members. Different models available in the literature for the deflection calculation of steel and FRP RC members are examined.

The effects of varying the cross-section dimensions (height and width), reinforcement ratio, reinforcement modulus of elasticity, and concrete compressive strength on the load deflection behaviour of SMA RC beams are discussed. Varying the concrete compressive strength and the cross-section width are found to have minor effects on the I_e value. The parametric study indicated that the reinforcement ratio and reinforcement modulus of elasticity have a significant effect on I_e. Moreover, the accuracy of the examined models for calculating deflection values is found to mainly depend on these two parameters.

The results of the parametric study are used to evaluate the applicability and accuracy of existing models to predict the deflection of SMA RC members. Statistical tools including *RMSE* and *AGE* showed that the model proposed by Bischoff (2007b) has the best performance for beams having reinforcement ratios greater than 0.6%. For lightly reinforced concrete beams ($\rho < 0.6\%$), Bischoff's model is un-conservative, and the ISIS design manual (2001) is found to be conservative for most of the studied sections and relatively accurate in predicting the deflection of SMA RC beams.

The limitation of the models examined in this paper underline the need for developing a new predictive tool for the deflection of SMA RC members, which can capture the effect of the reinforcement ratio and reinforcement modulus of elasticity, both at low and high reinforcement

ratios. An attempt is made in a companion paper to develop such a model using artificial intelligence.

REFERENCES

ACI 440.1R-03 2003. Guide for the design and construction of concrete reinforced with FRP bars. American Concrete Institute, Farmington Hills, Michigan, USA, 42 p.

ACI 440.1R-04 2004. Guide for the design and construction of concrete reinforced with FRP bars, proposed revision. American Concrete Institute, Farmington Hills, Michigan, USA, 35 p.

Alam, M.S., Youssef, M.A., and Nehdi, M. 2007. Utilizing shape memory alloys to enhance the performance and safety of civil infrastructure: a review. Canadian Journal of Civil Engineering, **34**(9): 1075-1086. doi: 10.1139/L07-038.

AS3600 2001. Australian standard for concrete structures. Standards Australia (SA), Sydney, Australia, 165 p.

Benmokrane, B., Chaallal, O., and Masmoudi, R. 1996. Flexural response of concrete beams reinforced with FRP reinforcing bars. ACI Structural Journal, **91**(2): 46–55.

Bischoff, P.H. 2007a. Rational model for calculating deflection of reinforced concrete beams and slabs. Canadian Journal of Civil Engineering, **34**(8): 992-1002. doi: 10.1139/L07-020.

Bischoff, P.H. 2007b. Effective moment of inertia for calculating deflections of concrete members containing steel reinforcement and fiber-reinforced polymer reinforcement. ACI Structural Journal, **104**(1): 68-75.

Branson, D.E. 1963. Instantaneous and time-dependent deflections of simple and continuous reinforced beams. Alabama Highway Research Report, Report No. 7, Alabama Highway Department, Bureau of Public Roads, Montgomery, Al, USA, 78 p.

Brown, V.L., and Bartholomew, C.L. 1996. Long-term deflections of GFRP-reinforced concrete beams. Proceedings, ICCI, Tucson, Arizona, 389–400.

CEB-FIP 1990. Model code for concrete structures. Comité Euro-International du Béton, Thomas Telford, London, UK.

Clark, P.W., Aiken, I.D., Kelly, J.M., Higashino, M. and Krumme, R.C. 1995. Experimental and analytical studies of shape memory alloy dampers for structural control. Smart Structures and Materials: Passive Damping, Proceedings of SPIE, 2445: 241-251.

CSA A23.3-04 2004. Design of concrete structures. Canadian Standards Association, Rexdale, Ontario, Canada, 240 p.

DesRoches, R. and Delemont, R. 2002. Seismic retrofit of bridges using shape memory alloys. Engineering Structures, **24**(3): 325-332. doi: 10.1016/S0141-0296(01)00098-0.

Elbahy, Y.I., Youssef, M.A., Nehdi, M., 2009, "Stress Block Parameters for Concrete Flexural Members Reinforced with Shape Memory Alloys", Materials and Structures, published online Nov. 2008. doi: 10.1617/s11527-008-9453-z.

El-Tawil, S., and Ortega-Rosales, J. 2004. Prestressing concrete using shape memory alloy tendons. ACI Structural Journal, **101**(6): 846-851.

Ghali, A., Hall, T., and Bobey, W. 2001. Minimum thickness of concrete members reinforced with fibre reinforced polymer bars. Canadian Journal of Civil Engineering, **28**(4): 583-592. doi: 10.1139/cjce-28-4-583.

Gilbert, R.I. 2006. Discussion of "reevaluation of deflection prediction for concrete beams reinforced with steel and fiber reinforced polymer bars." by Peter H. Bischoff. Journal of Structural Engineering, **132**(8): 1328-1330. doi: 10.1061/(ASCE)0733-9445(2006)132:8(1328).

Hall, T., and Ghali, A. 1997. Prediction of the flexural behaviour of concrete members reinforced with GFRP bars. Society for the Advancement of Material and Process Engineering (SAMPE), Proceedings of the 42nd International SAMPE Symposium and Exhibition, Anaheim, California, 1: 298-310.

Hall, T.S. 2000. Deflections of concrete members reinforced with fibre reinforced polymer (FRP) bars. M.Sc. Thesis, Department of Civil Engineering, The University of Calgary, Calgary, Alberta, Canada, 293 p.

ISIS Canada. 2001. Reinforcing concrete structures with fibre reinforced polymers. Design Manual 3. ISIS Canada Research Network, Winnipeg, Manitoba, Canada, 207 p.

Janke, L., Czaderski, C., Motavalli, M., Ruth, J. 2005. Applications of shape memory alloys in civil engineering structures - overview, limits and new ideas. Materials and Structures/Materiaux et Constructions, **38**(279): 578-592. doi: 10.1007/BF02479550.

Krumme, R., Hayes, J., and Sweeney, S. 1995. Structural damping with shape memory alloys: one class of devices. Smart Structures and Materials: Passive Damping, Proceedings of SPIE, 2445: 225-240.

Maji, A.K., and Negret, I. 1998. Smart prestressing with shape-memory alloy. Journal of Engineering Mechanics, **124**(10): 1121-1128. doi: 10.1061/(ASCE)0733-9399(1998)124:10(1121).

Mazzolani, F.M., Corte, G.D., and Faggiano, B. 2004. Seismic upgrading of RC building by means of advanced techniques: The ILVA-IDEM project. The proceedings of the 13th World Conference on Earthquake Engineering, Paper No. 2703, Vancouver, British Columbia, Canada.

Rangan, B.V. and Sarker, P.K. 2001. Bending stiffness of concrete flexural members reinforced with high strength steel. Code Provisions for Deflection Control in Concrete Structures, American Concrete Institute, SP203-09, 203: 143-156.

Saiidi, M.S., Sadrossadat-Zadeh, M., Ayoub, C., Itani, A. 2007. Pilot study of behavior of concrete beams reinforced with shape memory alloys. ASCE, Journal of Materials in Civil Engineering, **19**(6): 454-461. doi: 10.1061/(ASCE)0899-1561(2007)19:6(454).

Scanlon, A., Cagley Orsak, D.R., and Buettner, D.R. 2001. ACI code requirements for deflection control: a critical review. In code provisions for deflection control in concrete structures. Edited by E.G. Nawy and A. Scanlon, American Concrete Institute, Farmington Hills, Mich, SP-203: 1-14

Scott, B.D.; Park, R.; and Priestley, M.J.N. 1982. Stress-strain behavior of concrete confined by overlapping hoops at low and high strain rates. ACI journal, **79**(1): 13-27.

Stevens, N.J., Uzumeri, S.M., and Collins, M.P. 1987. Analytical modeling of reinforced concrete subjected to monotonic and reversed loading. Report No. 87-1, University of Toronto, Toronto, Ontario, Canada, 3634 p.

Tamai, H., Miura, K., Kitagawa, Y., Fukuta, T. 2003. Application of SMA rod to exposed-type column base in smart structural system. Proceedings, Smart Structures and Materials: Smart Systems and Nondestructive Evaluation for Civil Infrastructures, The International Society for Optical Engineering, 169-177. doi: 10.1117/12.482395.

Toutanji, H.A., and Saafi, M. 2000. Flexural behavior of concrete beams reinforced with glass fiber-reinforced polymer GFRP bars. ACI Structural Journal, **97**(5): 712-719.

Yost, J.R., Gross, S.P., and Dinehart, D.W. 2003. Effective moment of inertia for glass fiber-reinforced polymer-reinforced concrete beams. ACI Structural Journal, **100**(6): 732-739.

Youssef, M., and Ghobarah, A. 1999. Strength deterioration due to bond slip and concrete crushing in modeling of reinforced concrete members. ACI Structural Journal, **96**(6): 956-967.

Youssef, M.A., Alam, M.S., and Nehdi, M. 2008. Experimental investigation on the seismic behaviour of beam-column joints reinforced with superelastic shape memory alloys. Journal of Earthquake Engineering, **12**(7): 1205-1222. doi: 10.1080/13632460802003082.

Youssef, M.A., and Rahman, M. 2007. Simplified seismic modeling of reinforced concrete flexural members. Magazine of Concrete Research, **59**(9): 639-649. doi: 10.1680/macr.2007.59.9.639.

LIST OF SYMBOLS

AGE	Average algebraic error.
B	Cross-section width.
E	Modulus of elasticity of reinforcing bars.
$E_{cr\text{-}SMA}$	SMA modulus of elasticity in the austenite phase.
E_{FRP}	Modulus of elasticity of FRP.
E_{p2}	SMA modulus of elasticity in the martensite phase.
E_s	Modulus of elasticity of steel.
f_c	Concrete compressive stress.
f'_c	Concrete compressive strength.
f_{cr}	Cracking stress.
$f_{cr\text{-}SMA}$	SMA critical stress which represents the start of the martensite stress induced transformation.
f_{p1}	SMA martensite stress induced stress.
FRP	Fibre reinforced polymers.
f_{SMA}	SMA stress.
f_t	Concrete tensile stress.
$f_{u\text{-}SMA}$	SMA ultimate stress.
$f_{y\text{-}SMA}$	SMA yielding stress.
H	Cross-section height.
h'	Width of the concrete core measured to outside of the ties.

I_{cr}	Cracked moment of inertia.
I_e	Effective moment of inertia.
I_g	Un-cracked moment of inertia.
I_T	Un-cracked moment of inertia of the transformed section.
K_h	Confinement factor.
M	Order of the equation.
M_a	Applied moment.
M_{cr}	Cracking moment.
RC	Reinforced Concrete.
RMSE	Root mean square error.
S_h	Centre-to-centre spacing of the ties or hoop sets.
SMA	Shape memory alloy.
Z	Slope of concrete compressive strain softening branch.
A	Bond dependent coefficient.
B	Reduction factor.
ε_c	Concrete compressive strain.
ε_{cr}	Concrete cracking strain.
$\varepsilon_{cr\text{-}SMA}$	SMA critical strain.
ε_{cu}	Ultimate concrete strain.
ε_o	Concrete strain corresponding to the peak stress.
ε_{pl}	SMA martensite stress induced strain.
ε_{SMA}	SMA strain.

$\varepsilon_{u\text{-}SMA}$	SMA strain at failure.
$\varepsilon_{y\text{-}SMA}$	SMA yielding strain.
P	Reinforcement ratio.
ρ_b	Balanced section reinforcement ratio.
ρ_{FRP}	Reinforcement ratio of FRP RC section.
$\rho_{stirrups}$	Ratio of volume of stirrup reinforcement to volume of concrete core measured to outside of the stirrups.
Φ_{cr}	Cracking curvature.

Table 1: Materials properties

Material	Property	JBC1	JBC2
Concrete	Compressive Strength (MPa)	53.5	53.7
	Tensile Strength (MPa)	3.5	2.8
Longitudinal Steel	Yield Stress (MPa)	520	450
	Ultimate Strength	630	650
Transverse Steel	Yield Stress (MPa)	422	422
	Ultimate Strength (MPa)	682	682

Table 2: Details of analyzed sections

Section	Studied variables	h (mm)	b (mm)	A_{SMA} (mm^2)	ρ_{SMA} (%)	E_{SMA} (MPa)	f'_c (MPa)	L (mm)
C_1	h	400	300	1,200	1.11	40,000	45	6000
C_2	h	600	300	1,200	0.71	40,000	45	6000
C_3	h	800	300	1,200	0.53	40,000	45	6000
C_4	b	500	250	950	0.83	40,000	40	5000
C_5	b	500	400	950	0.52	40,000	40	5000
C_6	b	500	600	950	0.34	40,000	40	5000
C_7	ρ	500	250	460	0.40	40,000	40	5000
C_8	ρ	500	250	920	0.80	40,000	40	5000
C_9	ρ	500	250	1,380	1.20	40,000	40	5000
C_{10}	ρ	500	250	2,050	1.77	40,000	40	5000
C_{11}	E	500	250	800	0.70	30,000	40	5000
C_{12}	E	500	250	800	0.70	45,000	40	5000
C_{13}	E	500	250	800	0.70	65,000	40	5000
C_{14}	f_c'	600	300	1,100	0.65	40,000	20	6000
C_{15}	f_c'	600	300	1,100	0.65	40,000	35	6000
C_{16}	f_c'	600	300	1,100	0.65	40,000	55	6000

LIST OF FIGURE CAPTIONS

Fig. 1: (a) Stress-strain model for concrete in compression (Scott et al. 1982); (b) Stress-strain model for concrete in tension (Youssef and Ghobarah 1999); (c) Stress-strain model for SMA (Alam et al. 2007); and (d) Fibre model for a concrete section.

Fig. 2: (a) Reinforcement details of specimens JBC-1 and JBC-2 (Youssef et al. 2008); and (b) Ni-Ti stress-strain relationship.

Fig. 3: (a) Moment-curvature analysis for SMA and steel RC sections (JBC2); (b) Curvature distribution along the beam; and (c) Load-displacement (Moment-area method vs. Experimental).

Fig. 4: Moment curvature relationships for un-cracked section, cracked section, and a cracked flexural member (Bischoff 2007a).

Fig. 5: Deflections calculated using moment-area method versus that of different models.

Fig. 6: Load-deflection relationship for SMA RC members. (a) Effect of cross-section height; (b) Effect of cross-section width; (c) Effect of reinforcement ratio; (d) Effect of reinforcement modulus of elasticity; and (e) Effect of concrete compressive strength.

Fig. 7: Moment-area deflection versus that calculated using different equations. (a) Benmokrane et al.'s Equation; (b) Brown and Bartholomew's Equation; (c) ACI 440.1R-03 Equation; (d) ACI 440.1R-04 Equation; (e) Yost et al.'s Equation; (f) ISIS Equation; (g) Bischoff's Equation; and (h) Branson's Equation;

Fig. 8: Evaluation of the accuracy of different models. (a) *RMSE* for predicted deflections using different models; and (b) *AGE* for predicted deflections using different models.

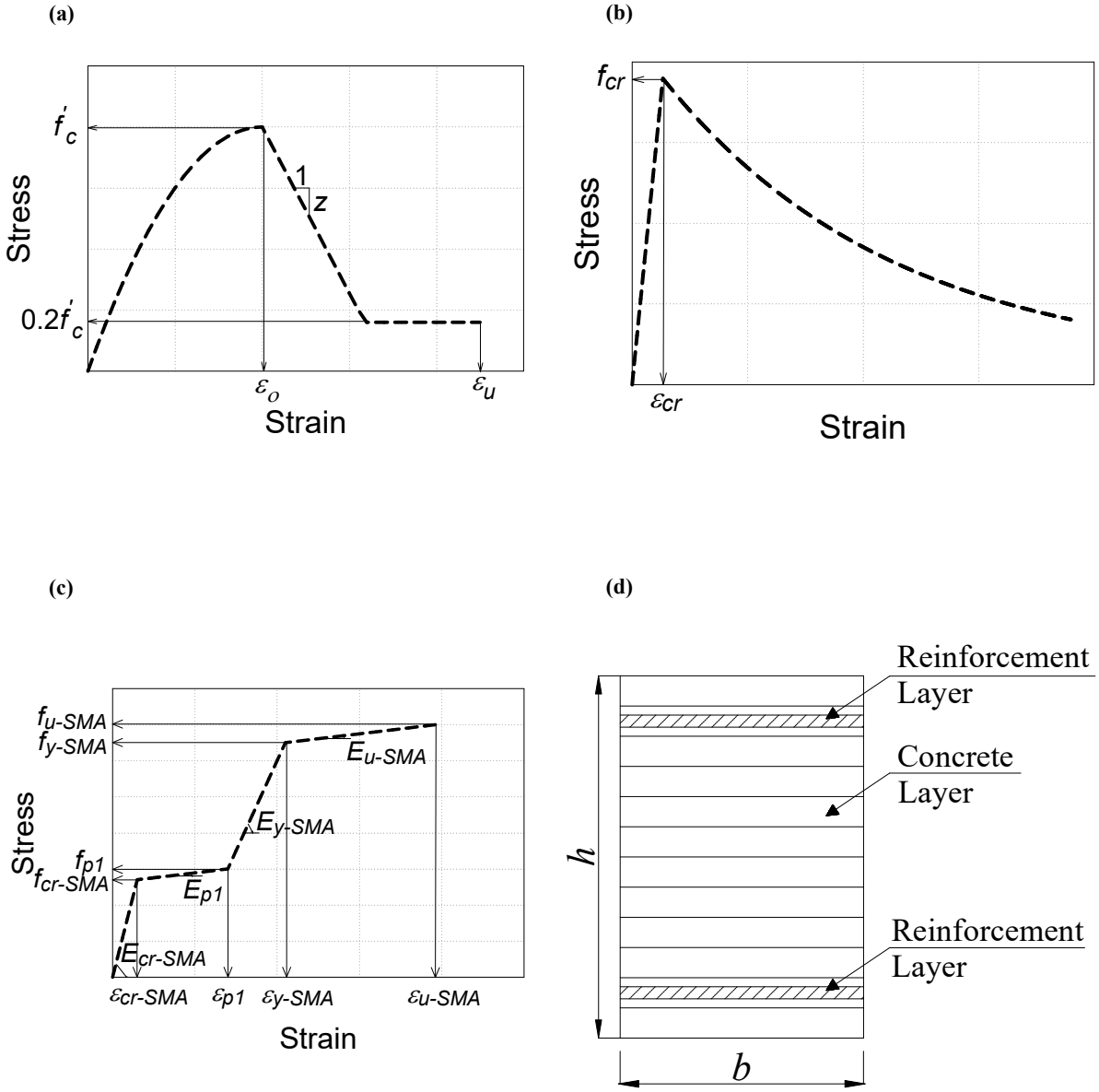
(a)
f'_c
1
z
Stress
$0.2f'_c$
ε_o
ε_u
Strain
(b)
f_{cr}
Stress
ε_{cr}
Strain
(c)
$f_{u\text{-}SMA}$
$f_{y\text{-}SMA}$
$E_{u\text{-}SMA}$
$E_{y\text{-}SMA}$
Stress
f_{p1}
$f_{cr\text{-}SMA}$
E_{p1}
$E_{cr\text{-}SMA}$
$\varepsilon_{cr\text{-}SMA}$
ε_{p1}
$\varepsilon_{y\text{-}SMA}$
$\varepsilon_{u\text{-}SMA}$
Strain
(d)
Reinforcement Layer
Concrete Layer
Reinforcement Layer
h
b

(a)

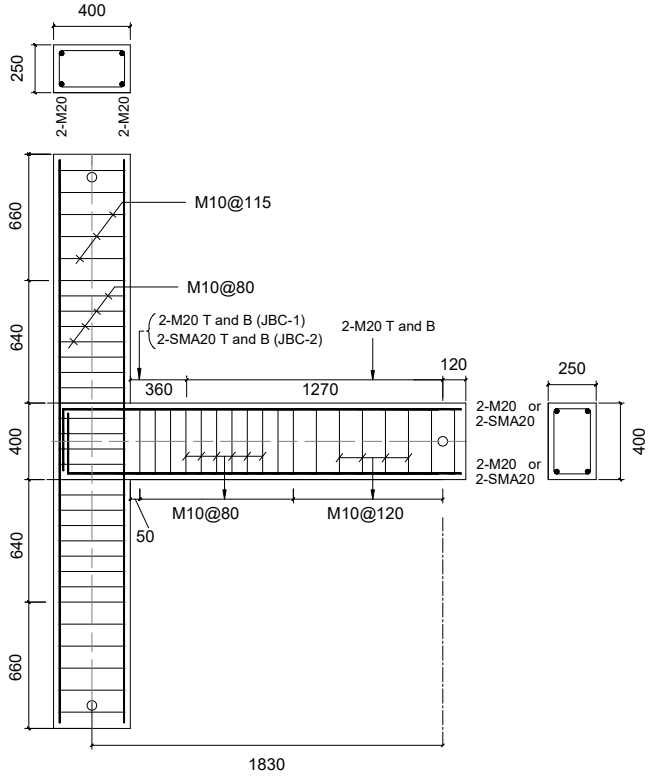
400
250
2-M20
2-M20
660
M10@115
M10@80
640
2-M20 T and B (JBC-1)
2-SMA20 T and B (JBC-2)
2-M20 T and B
120
250
360
1270
2-M20 or
2-SMA20
400
400
2-M20 or
2-SMA20
640
M10@80
M10@120
50
660
1830

(b)

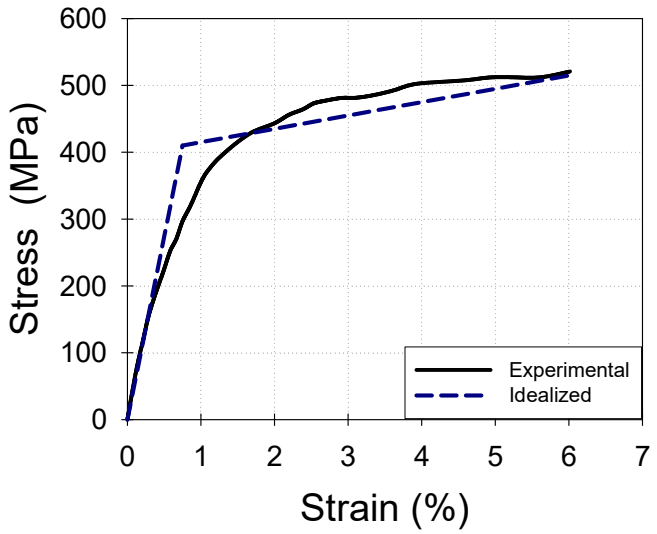
600
500
400
300
200
100
0
Stress (MPa)
0
1
2
3
4
5
6
7
Strain (%)
Experimental
Idealized

(a)

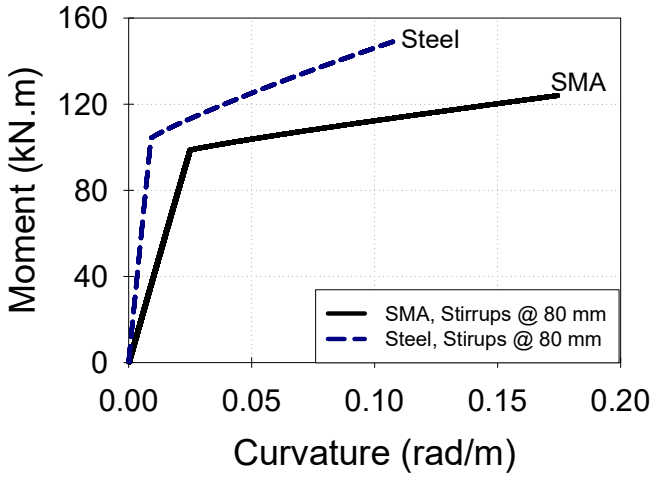
160
120
80
40
0
Moment (kN.m)
Steel
SMA
SMA, Stirrups @ 80 mm
Steel, Stirups @ 80 mm
0.00
0.05
0.10
0.15
0.20
Curvature (rad/m)

(b)

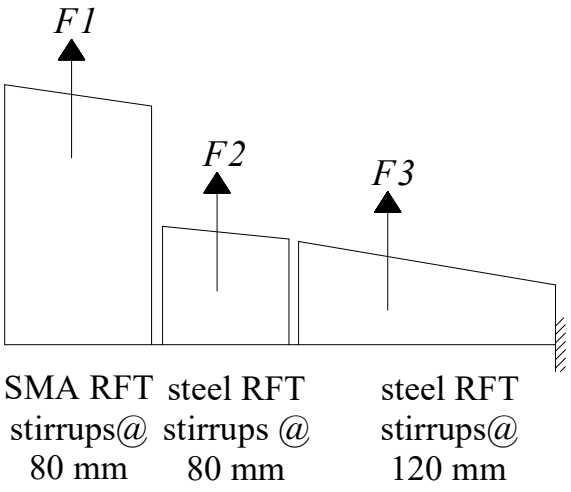
F1
F2
F3
SMA RFT stirrups@ 80 mm
steel RFT stirrups @ 80 mm
steel RFT stirrups@ 120 mm

(c)

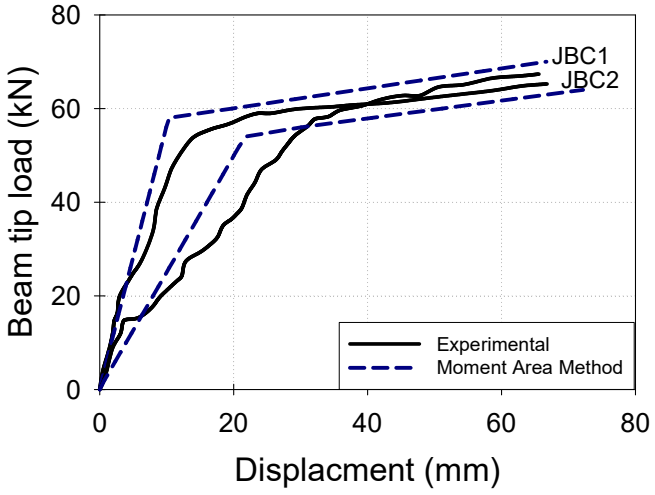
80
60
40
20
0
Beam tip load (kN)
JBC1
JBC2
Experimental
Moment Area Method
0
20
40
60
80
Displacment (mm)

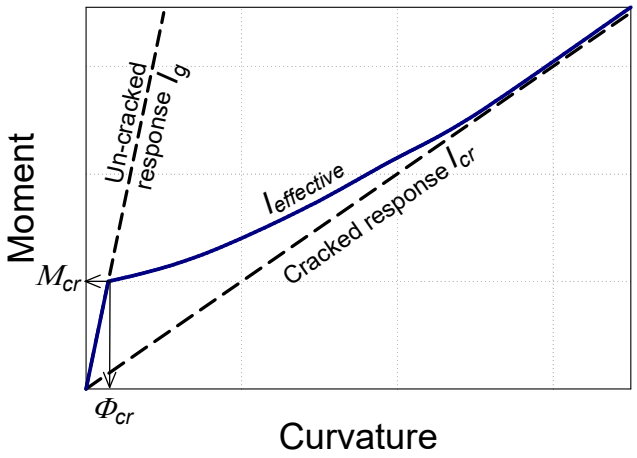
Moment
Curvature
Un-cracked response I_g
$I_{effective}$
Cracked response I_{cr}
M_{cr}
Φ_{cr}

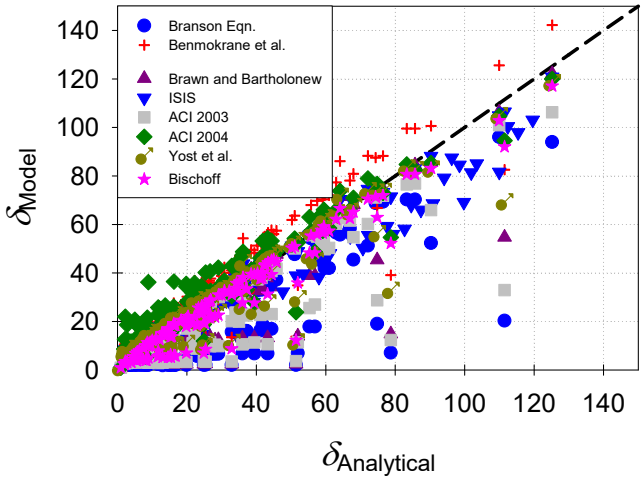
Branson Eqn.
Benmokrane et al.
Brawn and Bartholonew
ISIS
ACI 2003
ACI 2004
Yost et al.
Bischoff
0
20
40
60
80
100
120
140
δModel
δAnalytical

(a)

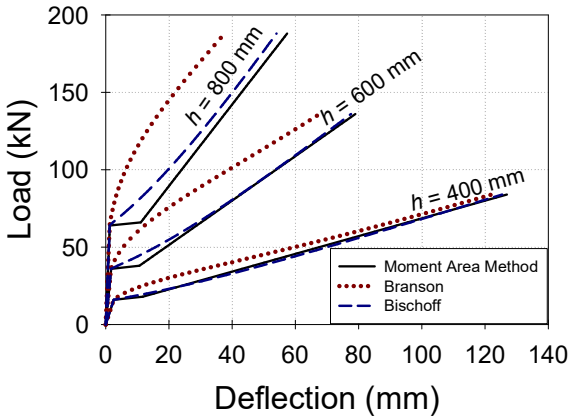
Load (kN)
Deflection (mm)
h = 800 mm
h = 600 mm
h = 400 mm
Moment Area Method
Branson
Bischoff

(b)

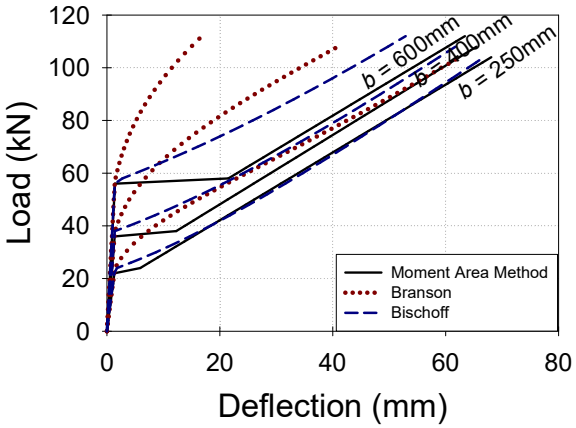
Load (kN)
Deflection (mm)
b = 600mm
b = 400mm
b = 250mm
Moment Area Method
Branson
Bischoff

(c)

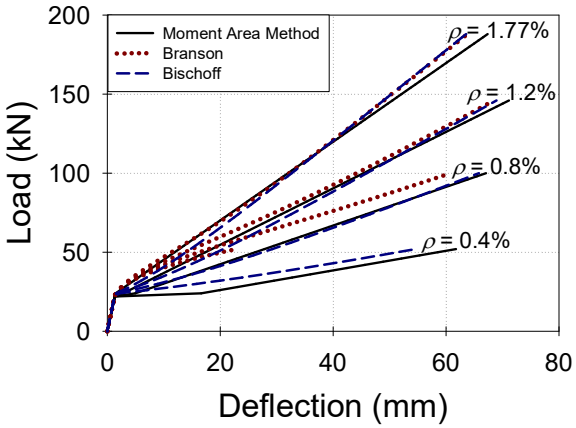
Load (kN)
Deflection (mm)
ρ = 1.77%
ρ = 1.2%
ρ = 0.8%
ρ = 0.4%
Moment Area Method
Branson
Bischoff

(d)

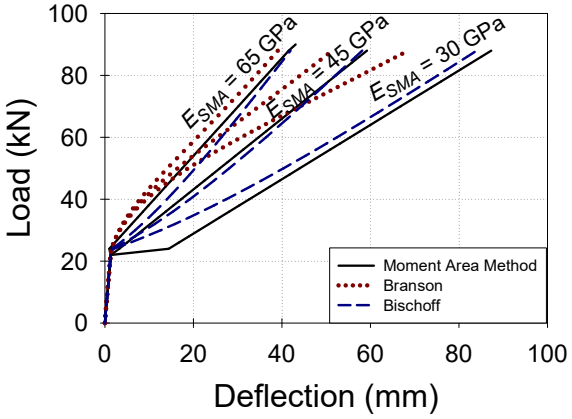
Load (kN)
Deflection (mm)
E_SMA = 65 GPa
E_SMA = 45 GPa
E_SMA = 30 GPa
Moment Area Method
Branson
Bischoff

(e)

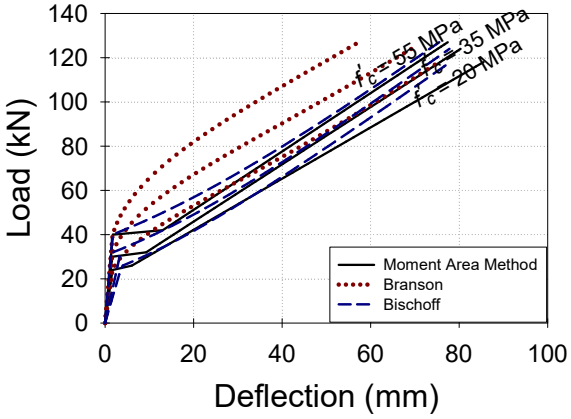
Load (kN)
Deflection (mm)
f'c = 55 MPa
f'c = 35 MPa
f'c = 20 MPa
Moment Area Method
Branson
Bischoff

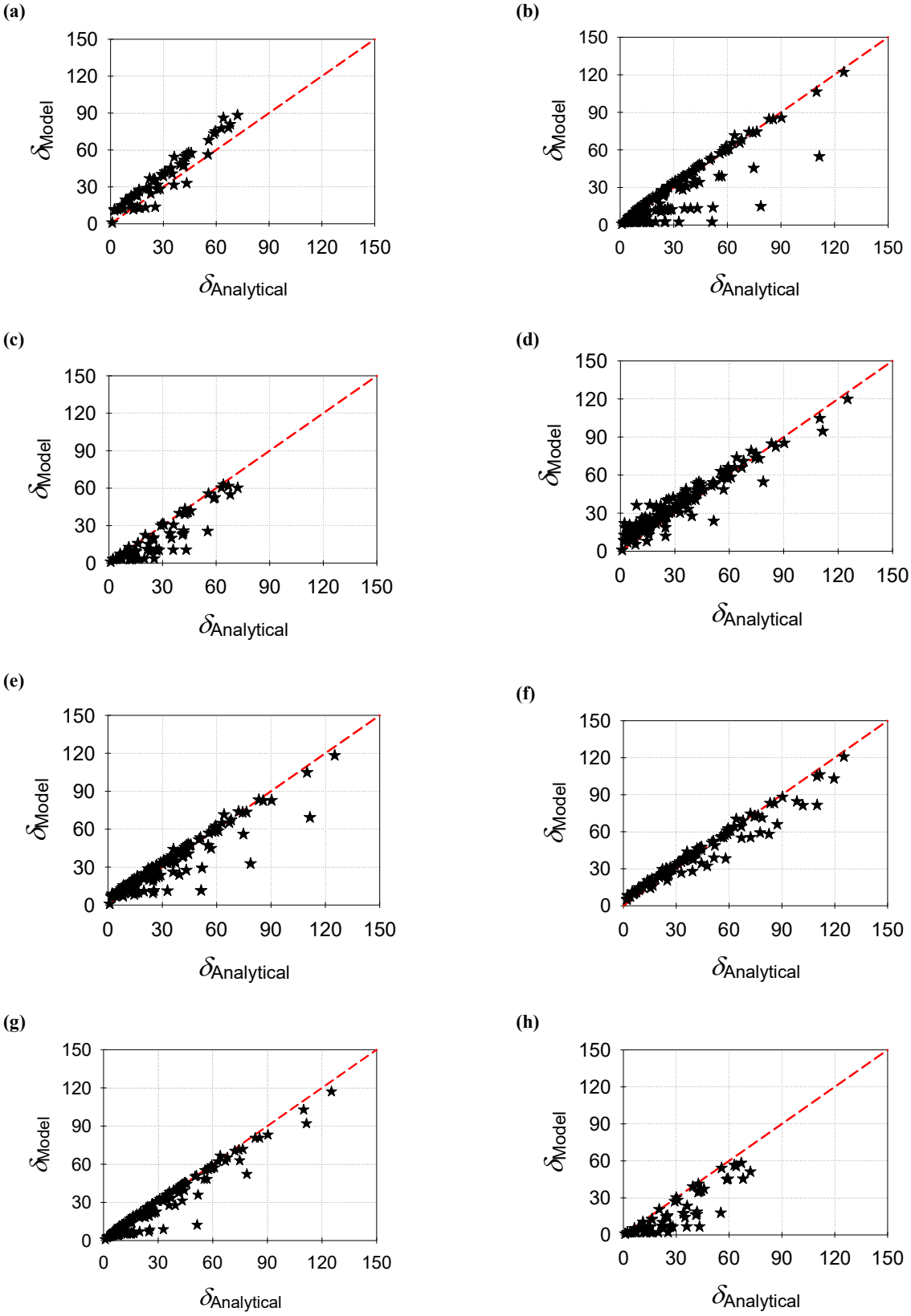
(a)
(b)
(c)
(d)
(e)
(f)
(g)
(h)
δ_{Model}
$\delta_{Analytical}$
0
30
60
90
120
150

(a)

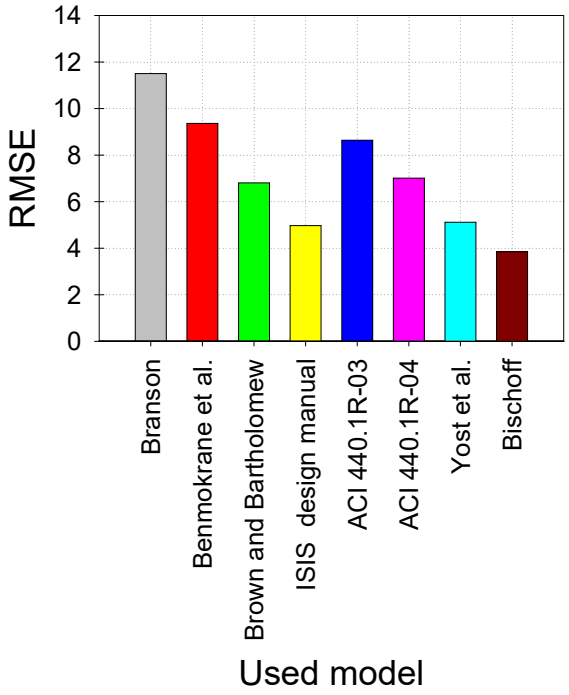
RMSE
14
12
10
8
6
4
2
0
Branson
Benmokrane et al.
Brown and Bartholomew
ISIS design manual
ACI 440.1R-03
ACI 440.1R-04
Yost et al.
Bischoff
Used model

(b)

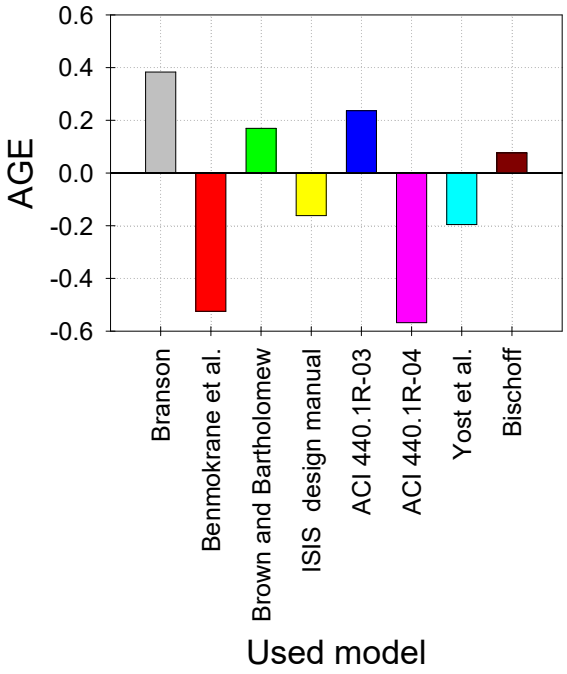
AGE
0.6
0.4
0.2
0.0
-0.2
-0.4
-0.6
Branson
Benmokrane et al.
Brown and Bartholomew
ISIS design manual
ACI 440.1R-03
ACI 440.1R-04
Yost et al.
Bischoff
Used model